This article has been accepted for publication in a future issue of this journal, but has not been fully edited. Content may change prior to final publication. Citation information: DOI 10.1109/TVT.2018.2880158, IEEE Transactions on Vehicular Technology

A Markovian Model for Analyzing Opportunistic Request Routing in Wireless Cache Networks

J. Dinal Herath, Anand Seetharam
Department of Computer Science, SUNY Binghamton, USA
jherath1@binghamton.edu, aseethar@binghamton.edu

***Abstract*—In this paper, we investigate the request routing delay of opportunistic routing for cache-enabled wireless networks considering uncorrelated and temporally correlated wireless channels. We model wireless channel variation at different time scales via two approaches—*i)* an abstract modeling approach where we model the variation considering Rayleigh fading and shadowing channel models, and *ii)* an empirical approach where the variation is modeled directly using signal strength measurements. We develop Markovian models to analyze the performance of opportunistic forwarding, leverage the wireless channel models to determine the packet transmission success probabilities and then utilize them to obtain the request routing delay. We first perform numerical experiments and simulations considering Rayleigh fading and shadowing channel models and then conduct a trace-based evaluation using signal strength measurements collected over a wireless sensor network testbed. Our experiments demonstrate the validity and effectiveness of our Markovian model in determining the request routing delay in real-world settings. Our work takes a step forward in providing network operators a tool for analyzing network performance before deploying their networks.**

I. Introduction

To address the explosive growth of mobile wireless traffic in recent years, content caching at storage-enabled in-network nodes has been proposed [13], [20]. By placing content at in-network nodes, requests for content can be served from en route caches in addition to the content custodian (origin server), thus improving user performance. Alongside this increase in data access traffic, recent years have also seen the emergence of various forwarding strategies that exploit the broadcast nature of the wireless medium [1], [17]. In a wireless network, when a node transmits a packet, multiple nodes in its vicinity can receive a copy of it and can participate in forwarding the packet toward the destination. A popular forwarding strategy is opportunistic routing. In opportunistic routing, if several nodes receive the same packet, an appropriate relay is selected for the next transmission of that packet.

In this paper, we analyze the request routing delay in cache-enabled wireless networks that forward requests following an opportunistic routing policy. Analyzing the performance of opportunistic routing in wireless cache networks is a relatively unexplored domain. Existing work related to our research can be separated into two categories—*i)* work related to opportunistic routing, *ii)* work related to caching or content placement. Most work in these two categories has primarily focused on developing novel opportunistic routing policies or designing better caching or content placement strategies, while performance analysis of opportunistic routing or caching policies in wireless settings considering realistic channel models has received limited attention.

In this paper, we consider cache-enabled wireless networks (e.g., cache-enabled heterogeneous networks, ad hoc networks, mesh networks, D2D networks) where users send requests for content that is always available at a content custodian, but may also be present at multiple in-network caches. We assume that the network uses a simple greedy opportunistic routing strategy to forward requests for content from users [1], [4]. In greedy opportunistic forwarding, if multiple nodes receive the same copy of the request, the node closest to the custodian forwards the request.

To investigate the performance of opportunistic routing in wireless cache networks, we model the wireless channel as a good-bad channel. A request transmission is successful if the channel is in the good state and unsuccessful otherwise. Prior work [28], [29] has demonstrated that a good-bad channel is an appropriate model to capture the successful/unsuccessful transmission of packets for temporally uncorrelated and correlated wireless channels, the two channel models we consider in our analysis. We describe these two models next.

i) Temporally uncorrelated wireless channels, where the channel state obtained for each request transmission is independently and identically distributed.
ii) Temporally correlated wireless channels, where the channel state transitions are modeled as a Markov chain.

Depending on the environment and the time scale at which the request transmissions occur, different channel models can be adopted to capture these variations. We model the received power variations over the channel using *i)* a Rayleigh fading channel model where the received power is modeled as an exponentially distributed random variable. For correlated channels, the temporal correlation is modeled as a modified Bessel function of the first kind and zeroth order and the state transition probabilities of the Markovian model are derived based on [28], [29]. *ii)* a shadowing channel model where the impact of shadowing on received power is modeled as a log-normally distributed random variable. For correlated channels, we model the autocorrelation function as being exponentially distributed and leverage it to design a good-bad Markovian

This article has been accepted for publication in a future issue of this journal, but has not been fully edited. Content may change prior to final publication. Citation information: DOI 10.1109/TVT.2018.2880158, IEEE Transactions on Vehicular Technology

channel model and determine the transition probabilities [19]. *iii)* an empirical approach, where the probabilities are calculated by directly measuring the changes in signal strength for both uncorrelated and correlated channels.

We design Markovian models to analytically determine the request routing delay for greedy opportunistic forwarding for the single flow case (i.e., satisfying requests for content from a single user to the custodian) for both uncorrelated and temporally correlated channel models. We derive expressions for the transition probabilities of the Markov chain for both scenarios and use them to determine the request routing delay.

We first conduct numerical experiments and simulations considering Rayleigh fading and shadowing channel models and then conduct a trace-based evaluation on publicly available signal strength measurement traces collected over a wireless sensor network testbed [10] to validate the usefulness of our Markovian models and to draw valuable insight into network performance. Our experiments show that the simulation and numerical results match closely for Rayleigh fading and shadowing channels as well as real-world signal strength measurements, which demonstrates the effectiveness of our Markovian model.

As expected, we observe that the request routing delay decreases as the cache capacity at individual nodes increases. Interestingly, we observe that benefit of caching is higher at lower values of packet success probability, primarily because it is easier to reach an in-network cache instead of the custodian in a few transmissions. We also observe that the delay of opportunistic routing increases as channel correlation increases. The main reason is that in case of correlated channels, while opportunistic routing requires a node to transmit multiple times over a poor channel to get the request through to downstream relays, it fails to take advantage of good channel conditions. This is in contrast to the uncorrelated case, where nodes get independent channel quality in different time slots.

The rest of the paper is organized as follows. We begin with a discussion of related work in Section II. We outline the network model and problem statement in Section III and then present the wireless channel models in Section IV. The Markovian model designed for analyzing the request routing delay is described in Section V. We present numerical and simulation results as well as experimental results on real-world signal strength measurements in Section VI. We conclude the paper with an outlook toward future work in Section VII.

II. Related Work

Our current work builds on our prior work [4], [18]. In [4], we only consider uncorrelated fading channels and compare the performance of opportunistic and cooperative routing strategies. In [18], we consider correlated fading channels and analyze the performance of greedy opportunistic routing for a simple four node network. In contrast to our previous work, the main difference in this work is that we consider the presence of in-network caches and consider uncorrelated and correlated fading and shadowing channel models [19], [28], [29] to analyze the performance of opportunistic request routing of a single flow in a general network. We also test the efficacy of our models on signal strength measurements collected over a wireless sensor network testbed. We note that presence of in-network caching adds a new dimension to this problem because a request can be satisfied by network nodes in addition to the custodian.

We next outline research related to opportunistic routing and caching in wireless networks and contrast it with our work. Chakchouk identifies different classes of opportunistic routing policies namely, geographic, link-state-aware, probabilistic, optimization-based and cross-layer [3]. Apart from traditional networks such as mesh and ad hoc [1], [4], [17], [18], recently, opportunistic routing has also been applied to new domains such as vehicular and underwater networks [7], [15]. The opportunistic routing policy analyzed in this paper is a greedy opportunistic routing strategy that combines ideas from both geographic and link-state-aware routing. In comparison to our work, most existing work related to design and analysis of opportunistic routing policies consider uncorrelated wireless channel models [5], [6], [8], [21].

Kim *et. al* propose a general framework for accurately capturing link correlation [14] by leveraging Signal to Interference plus Noise Ratio (SINR) whereas [27] takes a step further in proposing a model with the ability to predict link correlation in low power wireless networks. Wang *et. al* [23] design an opportunistic routing scheme that improves performance by exploiting the diversity of low correlated links. Additionally, a recent work [22] has shown that on expectation, link correlation-aware opportunistic routing policies perform better than link correlation-unaware opportunistic routing policies, thus, increasing the utility in analyzing opportunistic routing amidst channel correlation.

Analyzing the performance gains of in-network caching for opportunistic forwarding in wireless networks is limited. Most work related to caching in wireless networks focus on heterogeneous cellular networks comprising of a cellular infrastructure and few cache-enabled femtocells [9], [20], [25]. The primary goal in these papers is to find the best content placement strategy to minimize delay subject to some network constraints. In contrast to prior work, our goal is *not* to propose a new opportunistic routing strategy or to find the optimal content placement in a network, but rather to develop models to analyze the performance of wireless cache networks considering uncorrelated and correlated wireless channel models.

III. Network Model

We consider a stationary wireless network of N nodes consisting of a single user r_1, a content custodian r_N and $N-2$ cache-enabled nodes in between as shown in Figure 1. $\mathbb{N}$ thus denotes the set of all nodes. We assume that r_1 periodically sends requests for content that is permanently housed at r_N. Without loss of generality, we assume that the network nodes are numbered in terms of the distance from r_N, and that r_1 is located farthest away from r_N. Therefore, $\{r_1, r_2, ...r_{N-1}, r_N\}$ denotes the ordering of the nodes in terms of their distance from r_N, and is known apriori. We denote the distance between any two nodes r_i and r_j by d_{ij}. Figure 1 also shows the possible transmission probabilities

This article has been accepted for publication in a future issue of this journal, but has not been fully edited. Content may change prior to final publication. Citation information: DOI 10.1109/TVT.2018.2880158, IEEE Transactions on Vehicular Technology

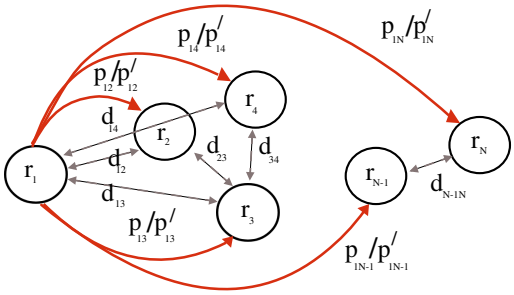

Fig. 1: An N node general network

(p_{1j} or p'_{1j}) between r_1 and the other network nodes for uncorrelated and correlated wireless channels, respectively.

We consider a content universe of size K. We assume that r_1 does not have any local cache, and all other network nodes except the custodian are provided with a cache of size C ($C < K$). We assume that content popularity varies according to some known distribution (e.g., Zipfian distribution). Let q_i denote popularity of the i^{th} piece of content (i.e., the probability of the user requesting content i).

We assume that the network adopts some content placement strategy (i.e., static caching) that determines the set of content to be placed at the network caches. The literature is rife with different kinds of content placement strategies [2], [9], [20]. For example, a widely adopted approach is to push popular content closer to the user so as to maximize performance.

We assume that the network adopts an opportunistic routing strategy to forward requests from the user to the custodian. Therefore, there is no notion of a fixed path between the user and the custodian. Due to broadcast nature of the wireless medium, nodes can overhear transmissions and can participate in forwarding the request toward the custodian. We assume that nodes forward requests based on a *greedy opportunistic routing policy*. In this strategy, if multiple nodes receive a copy of the request, the node closest to the custodian is always selected to transmit the request. Therefore, the node ordering $\{r_1, r_2, ...r_{N-1}, r_N\}$ also represents the priority for transmitting the request for greedy opportunistic routing. Formally, we denote "$r_i \succ r_j$" to represent that r_i has a higher priority than r_j. We note that there are several proposals [1], [17] that address implementation details, such as how to select the appropriate relay when multiple nodes overhear the transmission. However, we abstract away these details and focus on analyzing a simple implementation to appreciate the benefits of opportunistic routing in a cache network.

A. Problem Statement

Considering the network model described above, we address the following problem in this paper. *For a given content placement at in-network nodes for a cache-enabled wireless network, our goal in this paper is to design simple models to analyze the request routing delay for a greedy opportunistic routing strategy for realistic uncorrelated and correlated wireless channel models.* We next discuss the different wireless channel models considered in this paper.

IV. Wireless Channel Model

In order to analyze the performance of greedy opportunistic routing, we model the wireless channel in a binary manner as a good-bad channel. We assume that a request transmission between nodes r_i and r_j is successful if the Signal to Noise Ratio (SNR) is above a threshold β where $\beta > 0$. We consider both uncorrelated and temporally correlated wireless channels as shown in Figures 2(a) and 2(b) respectively. For uncorrelated channels, the channel state obtained for each request transmission is assumed to be independently and identically distributed. Let p_{ij} denote the probability of a successful transmission between nodes r_i and r_j for uncorrelated channels. For temporally correlated wireless channels, the next channel state is assumed to be dependent on the current channel state and the state transitions are modeled as a Markov chain. Therefore, for correlated channels, the transition matrix capturing this correlation is of the form

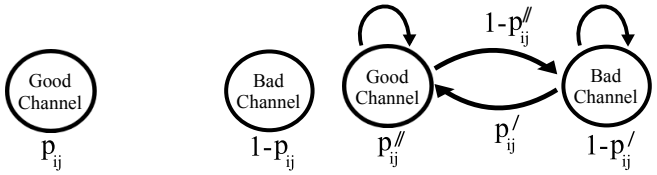

(a) Uncorrelated channel (b) Correlated channel

Fig. 2: Wireless Channel Models

$$M = \begin{bmatrix} P[success|success] & P[failure|success] \\ P[success|failure] & P[failure|failure] \end{bmatrix} \quad (1)$$

We denote $P[success|failure]$ by p'_{ij} and $P[success|success]$ as p''_{ij}. In this paper, we consider that only a single request is in transit between source and custodian and so we are primarily interested in the probability p'_{ij}. We determine the probabilities p_{ij} and p'_{ij} analytically as well as empirically. In the analytical approach, we model the wireless channel as *i)* a Rayleigh fading channel, and *ii)* a Lognormal shadowing channel. Depending on the environment and the time scale at which request transmissions occur, one model might be more suitable than the other. In the empirical approach, the probabilities are calculated by directly measuring the changes in signal strength for both uncorrelated and correlated channels.

For our analytical approach, we model the SNR (S_{ij}) for a single transmission between nodes r_i and r_j to be given by

$$S_{ij} = \frac{L\, P\, d_{ij}^{-\alpha}}{N_0} \quad (2)$$

where N_0 is the constant background noise, P the transmitted power at r_i, α the path loss exponent, d_{ij} the distance between the nodes and L the random attenuation component caused due to multipath fading or shadowing depending on the timescale.

A. Rayleigh fading channel

1) Uncorrelated fading channel: For Rayleigh fading, L is the Rayleigh fading coefficient and we model it as an exponentially distributed random variable with mean 1. For uncorrelated channels, we assume L is independently and identically distributed (i.i.d) in different time slots. Therefore,

This article has been accepted for publication in a future issue of this journal, but has not been fully edited. Content may change prior to final publication. Citation information: DOI 10.1109/TVT.2018.2880158, IEEE Transactions on Vehicular Technology

$$p_{ij} = \exp\left(\frac{-\beta N_0}{P\, d_{ij}^{-\alpha}}\right) \tag{3}$$

2) Correlated fading channel: Temporal correlation in a wireless channel can occur in scenarios where the coherence time for a channel is large, thus causing the channel to be correlated across time slots. We model the fading correlation as a modified Bessel function of the first kind and zeroth order [28], [29]. Zorzi *et al.* demonstrate using an information-theoretic approach that for a block error process, a Markovian model is reasonable when fading correlation is taken into account [28], [29]. This indicates that a success or a failure of a transmission between a pair of nodes in a given time slot can be modeled dependent solely on the result of the previous transmission. From [29], the conditional probability of success given failure between nodes r_i and r_j is given by,

$$p_{ij}^{'} = \frac{Q(\theta, \rho\theta) - Q(\rho\theta, \theta)}{\exp(b_{ij}) - 1} \tag{4}$$

In equation 4, $Q(:,:)$ is a Marcum Q function, ρ is the channel correlation coefficient which is given by a modified Bessel function of the first kind of zeroth order, $\theta = \sqrt{\frac{2b_{ij}}{1-\rho^2}}$ and $b_{ij} = \frac{\beta N_0}{P d_{ij}^{-\alpha}}$.

B. Shadowing channel

1) Uncorrelated shadowing channel: In case of shadowing, L is modeled as a lognormally distributed random variable [16]. Assuming $X = log(L)$, X is modeled as $N(0, \sigma^2)$. Therefore, p_{ij} for a shadowing channel is given by,

$$p_{ij} = \frac{1}{2}\left(1 - erf\left(\frac{\beta^{'}}{\sigma\sqrt{2}}\right)\right) \tag{5}$$

where $\beta^{'} = log\left(\frac{\beta N_0}{P\, d_{ij}^{-\alpha}}\right) = log(b_{ij})$.

2) Correlated shadowing channel: For correlated wireless channels, we model the temporal autocorrelation of shadowing to be exponential [12], [24], [26]. An exponential autocorrelation function means that shadowing forms an AR(1) process which in turn means that it can be modeled as a Markov process [19]. We assume that the entire range of shadowing is divided into two states Y_0 and Y_1, where Y_0 and Y_1 denote the range of shadowing that indicate transmission failure ($X < \beta^{'}$) and success ($X \geq \beta^{'}$) respectively. Therefore, $p_{ij}^{'}$ for a shadowing channel is given by,

$$p_{ij}^{'} = P\left[X_{k+1} \in Y_1 \mid X_k \in Y_0\right] \tag{6}$$

Following [19], we derive $p_{ij}^{'}$ as,

$$\begin{aligned} p_{ij}^{'} &= P\left[X_{k+1} \in Y_1 \mid X_k \in Y_0\right] \\ &= \frac{\int_{Y_0}\int_{Y_1} f_{X_{k+1}|X_k}\left(x_{k+1} \mid x_k\right) dx_{k+1} f_{X_k}\left(x_k\right) dx_k}{\int_{Y_0} f_{X_k}\left(x_k\right) dx_k} \\ &= \frac{\int_{Y_0}\left(1 - erf\left(\frac{\beta^{'} - \rho x_k}{\sigma\sqrt{2(1-\rho^2)}}\right)\right) f_{X_k}\left(x_k\right) dx_k}{1 + erf\left(\frac{\beta^{'}}{\sigma\sqrt{2}}\right)} \end{aligned} \tag{7}$$

where ρ denotes the autocorrelation between two successive samples. We note that when $\rho = 0$ equation 7 degenerates into equation 5.

C. Empirical Approach

The transmission probabilities between nodes can also be determined by performing signal strength measurements at the receiving nodes. Since the channel is modeled in a binary manner, successful and unsuccessful transmissions can be mapped to 1 and 0 respectively. For an uncorrelated channel, p_{ij} can be calculated simply as the fraction between the number of total successful requests from node r_i to r_j over the total number of requests between them. For a correlated channel, $p_{ij}^{'}$ can be computed as the fraction between the number of successes given a failure in the request stream over the total number of successes and failures given a failure in the request stream between nodes r_i and r_j.

V. Analytical Framework

In this section, we formulate Markovian models for analyzing the request routing delay using greedy opportunistic routing in cached-enabled networks for uncorrelated and correlated wireless channels. We consider the single request case, i.e., the user sends a new request only after its previous request has been satisfied. Each request is initiated by the user and is forwarded by in-network nodes until it reaches the custodian or some en route node that has a cached copy of the requested content. As mentioned earlier, we assume that the set of content in a node's cache is determined by a content placement strategy. Let H_f denote the set of nodes that have the copy of content f. Note that H_f thus includes the custodian. We next design the Markovian model and present its transition matrix for uncorrelated and correlated wireless channels for the general network considered in Figure 1. However, for the sake of understanding, we explain the model using a simple 4 node network.

A. Uncorrelated Channel

For constructing the Markovian model, we first consider the different states in which a network node could be in for a request in transit. For the uncorrelated channel, each node can be in two states - 0 and 1. State 1 denotes the state of a network node if it is going to transmit the request in the next time slot. State 0 captures two scenarios - *i)* the node has not received the request, *ii)* the node has received the request, but is not participating in retransmitting this request as some other higher priority node has also received the same request. For cases where a cache hit occurs at an intermediate node, we assume that the content is served immediately. Therefore, as explained in the four node example below such nodes do not partake in active retransmission, which subsequently reduces the state space of the Markovian model.

The set of nodes H_f where the content is available being dependent on f, we need to construct a separate Markov chain for each content f. For content f, we denote the state of the network using an n-tuple that captures the active relay for the request in the next time slot. For a four node network, the Markov chain could consist of maximum four states, namely

This article has been accepted for publication in a future issue of this journal, but has not been fully edited. Content may change prior to final publication. Citation information: DOI 10.1109/TVT.2018.2880158, IEEE Transactions on Vehicular Technology

$A_1 = (1,0,0,0)$, $A_2 = (0,1,0,0)$, $A_3 = (0,0,1,0)$, and $A_4 = (0,0,0,1)$. A_4 denotes the state where the request is served which could happen if the request reaches the custodian or some intermediate node that has a cached copy of the content. Additionally, depending on the set of nodes that cache a copy of the content, transitions to and from certain states may not be possible. For example, if we consider that content f is cached at r_3, transitioning to and from state A_3 is not possible because if r_3 receives the request, the network will transition to state A_4 as the request has been satisfied. Therefore, one can remove these states (in this case A_3) from the Markov chain for content f. Recall that we assume that the user transmits a new request after a request has been satisfied. Therefore, when the network transitions to state A_4, (i.e., the request is satisfied), the state transition in the next time step will correspond to the states reachable from the user with the respective probabilities.

Extending the above logic to a network of N nodes, the Markov chain will consist of $N - H_f + 1$ states (A_i, $\forall i = 1$ to $N, r_i \notin H_f - r_N$). Having designed the Markov chain, the next step is to derive its transition matrix. Let P_{ij}^f represent the transition from state A_i to A_j, ($\forall i,j = 1$ to $N, r_i, r_j \notin H_f - r_N$) for content f. Equation 8 shows the transition matrix for the Markov chain described above.

$$P_{ij}^f = \begin{cases} 0 & \text{if } i > j, \forall i < N \\ \prod\limits_{\substack{r_k \in N - H_f \\ r_k \succ r_j}} (1 - p_{ik}) \prod\limits_{r_k \in H_f} (1 - p_{ik}) & \text{if } i = j, \forall i < N \\ p_{ij} \prod\limits_{\substack{r_k \in N - H_f \\ r_k \succ r_j}} (1 - p_{ik}) \prod\limits_{r_k \in H_f} (1 - p_{ik}) & \text{if } i < j, \forall j < N \\ 1 - \prod\limits_{r_k \in H_f} (1 - p_{ik}) & \text{if } j = N, \forall i < N \\ p_{1j} & \text{if } i = N \end{cases} \tag{8}$$

B. Correlated Channel

For a correlated channel, we need to take into account the fact that an unsuccessful transmission of a request by a node in the previous time slot impacts the probability of successful transmission in the next time slot. To model this, we consider that each node can be in three states—0, 1 and 1^*. State 0 is similar to state 0 for the uncorrelated scenario. State 1 denotes that a node is going to transmit a request for the first time in the next time slot, while state 1^* denotes that a node failed to successfully transmit a request to any of the higher priority nodes in the previous time slot and is thus going to transmit it again in the upcoming time slot.

Once again, we consider a simple four node network to understand the different states of the Markov chain. The Markov chain can consist of maximum six states—$A_2 = (0,1,0,0)$, $A_3 = (0,0,1,0)$, $A_4 = (0,0,0,1)$ and $A_1' = (1^*,0,0,0)$, $A_2' = (0,1^*,0,0)$, $A_3' = (0,0,1^*,0)$. Every state in the Markov chain for the uncorrelated channel case except for A_1 and A_4 (i.e., the states that account for the user transmitting the request and the request getting satisfied in the network) has two corresponding states in the Markov chain for the correlated case. This takes into consideration the fact that a node can be in state 1 or 1^* when it serves as an active relay. For example, states A_2 and A_2' denote the cases when r_2 transmits a request for the first time and it retransmits the same request after a failed attempt respectively.

A_4 denotes the state that the request reaches the custodian or is satisfied by an en route cache while $A_1' = (1^*,0,0,0)$ denotes the state that the user transmits the request after a failed attempt. Note that the Markov chain does not need a state $A_1 = (1,0,0,0)$ as it is included in A_4. The state transition from A_4 correspond to the states reachable from the user when it transmits for the first time. Additionally, if the request transmission from the user to all other network nodes is unsuccessful, the Markov chain will transition to state A_1'. Therefore, if a state A_1 is included in the Markov chain, it will be unreachable from all other states and its steady state probability will be zero. Once again, states corresponding to the nodes that have a cached copy of the content (except the custodian) are not part of the Markov chain. For example, if r_3 has a cached copy of content f, then states A_3 and A_3' will not be part of the Markov chain. Extending the above analysis for an N node network, the Markov chain will consist of $2(N - H_f)$ states for content f, (A_i, $\forall i = 2$ to $N, r_i \notin H_f - r_N$; A_i', $\forall i = 1$ to $N-1, r_i \notin H_f$).

Once again, the next step is to derive the transition probabilities of the Markov chain. Recall that for the correlated channel case, equations 4 and 7 provide the conditional probability of successful request transmission in the current time slot given an unsuccessful request transmission in the previous time slot between nodes r_i and r_j. For ease of understanding, we split the transition probabilities into four separate pairs to cover the following cases - transitions from *i)* state A_i to state A_j, *ii)* state A_i to state A_j', *iii)* state A_i' to state A_j and *iv)* state A_i' to state A_j'. Equations 9, 10, 11 and 12 show the transition probabilities for cases *i, ii, iii and iv* for the correlated fading scenario for content f respectively. In general, these equations take care of the fact that transitions cannot take place from A_i to A_j (except when $i < j$) or from A_i to A_j' (unless $i = j$ or $i = N, j = 1$). Additionally, the equations also take care of fact that transitions to state A_N will occur if the request reaches the custodian or any intermediate in-network cache.

$$P_{ij}^{1f} = \begin{cases} 0 & \text{if } i \geq j, \forall i < N \\ p_{ij} \prod\limits_{\substack{r_k \in N - H_f \\ r_k \succ r_j}} (1 - p_{ik}) \prod\limits_{r_k \in H_f} (1 - p_{ik}) & \text{if } i < j, \forall j < N \\ 1 - \prod\limits_{r_k \in H_f} (1 - p_{ik}) & \text{if } j = N, \forall i < N \\ p_{1j} \prod\limits_{\substack{r_k \in N - H_f \\ r_k \succ r_j}} (1 - p_{1k}) \prod\limits_{r_k \in H_f} (1 - p_{1k}) & \text{if } i = N, \forall j < N \\ 1 - \prod\limits_{r_k \in H_f} (1 - p_{1k}) & \text{if } i,j = N \end{cases} \tag{9}$$

This article has been accepted for publication in a future issue of this journal, but has not been fully edited. Content may change prior to final publication. Citation information: DOI 10.1109/TVT.2018.2880158, IEEE Transactions on Vehicular Technology

$$P_{ij}^{2f} = \begin{cases} 0 & \text{if } i \neq j, \forall i < N \\ 0 & \text{if } i = N, \forall j \neq 1 \\ \prod\limits_{\substack{r_k \in N - H_f \\ r_k \succ r_j}} (1 - p_{ik}) \prod\limits_{r_k \in H_f} (1 - p_{ik}) & \text{if } i = j, \forall i < N \\ \prod\limits_{\substack{r_k \in N - H_f \\ r_k \succ r_j}} (1 - p_{1k}) \prod\limits_{r_k \in H_f} (1 - p_{1k}) & \text{if } i = N, j = 1 \end{cases} \tag{10}$$

$$P_{ij}^{3f} = \begin{cases} 0 & \text{if } i \geq j, \forall i < N \\ p'_{ij} \prod\limits_{\substack{r_k \in N - H_f \\ r_k \succ r_j}} (1 - p'_{ik}) \prod\limits_{r_k \in H_f} (1 - p'_{ik}) & \text{if } i < j, \forall i < N \\ 1 - \prod\limits_{r_k \in H_f} (1 - p'_{ik}) & \text{if } j = n, \forall i < N \end{cases} \tag{11}$$

$$P_{ij}^{4f} = \begin{cases} 0 & \text{if } i \neq j \\ \prod\limits_{\substack{r_k \in N - H_f \\ r_k \succ r_j}} (1 - p'_{ik}) \prod\limits_{r_k \in H_f} (1 - p'_{ik}) & \text{if } i = j \end{cases} \tag{12}$$

C. Delay Calculation

Having designed the Markovian models and derived their transition matrices for the uncorrelated and correlated cases, we leverage them to obtain expressions for the request routing delay. Let Π_i^f and $\Pi_i'^f$ denote the steady state probabilities for states A_i and A'_i for content f respectively. In our model, the expected delay D_f for a request for content f can be calculated as the inverse of the steady state probability of being in state A_N. Therefore, $D_f = \frac{1}{\Pi_N^f}$. Hence, the expected delay D for both uncorrelated and correlated scenarios is given by,

$$D = \sum_{f=1}^{K} q_f \frac{1}{\Pi_N^f} \tag{13}$$

VI. Experimental Evaluation

In this section, we first present numerical and simulation results for uncorrelated and correlated fading and shadowing channels and then conduct a trace-based evaluation on signal strength measurements collected over a wireless sensor network testbed to demonstrate that the proposed Markovian model performs well in a variety of different settings. We observe from our experiments that the numerical and simulation results match closely that demonstrates the validity and effectiveness of our Markovian models. We also conduct experiments to study the impact of different network parameters on delay.

For the results presented here, we assume equidistant placement of nodes. We assume that content popularity varies according to a Zipfian distribution with skewness parameter a. We assume that content is distributed according to the following strategy. We rank content based on popularity. Half of the cache capacity at each node is filled randomly from the top 20% content and the remaining capacity is filled from the bottom 80% content. This ensures that the most popular content is readily available in the network, but also allows in-network caching of less popular content.

We use the following default parameters in our experiments: number of network nodes including user and custodian $(N) = 4$, cache size at individual nodes $(C) = 10$, the content universe (K) = 100, the skewness parameter (a) = 0.8, the correlation coefficient (ρ) = 0.6 and the standard deviation for shadowing (σ) = 8. We conduct all experiments in MATLAB (simulations and numerical analysis) by varying the values of N, C, K, a, ρ and σ.

A. Experiments for Rayleigh Fading and Shadowing Channels

In this subsection, we compare numerical and simulation results for Rayleigh fading and shadowing channels. In our simulations, each data point is obtained over 10 runs of the experiment. For each simulation run, 10000 requests are sent from the user to the custodian and the delay is calculated as the average delay of all requests. Additionally, to take into account the content popularity in our simulations, we assume that user issues requests that are independently and identically distributed according to a Zipfian distribution. Each data point is then calculated as the average of 10 runs and the error bar shown around each data point is twice the standard deviation.

1) Closeness of Numerical and Simulation Results: Figures 3 and 4 show the variation in delay with the one hop success probability considering i.i.d. uncorrelated and correlated channels respectively for the default parameters for Rayleigh fading and shadowing. In these figures, we compare the results obtained via our numerical analysis and the simulations for different cache capacities. We observe from these figures that the numerical and simulation results match closely which demonstrates the validity and effectiveness of our Markovian models.

As expected, we observe that the delay decreases as the cache capacity increases. From a caching perspective, we observe that in-network caching has greater benefit for lower values of p. The reason is that for lower values of p, it is harder to reach the custodian in a few transmissions and thus having a cached copy of the content closer to the user helps in satisfying the request earlier. We observe that the delay decreases as the one hop success probability increases. We also observe that the delays obtained for shadowing are lower than fading for uncorrelated and correlated channels. This is because the transmission probability for fading (equation 3) is more sensitive to variations in distance in comparison to shadowing (equation 5). Therefore, the decrease in transmission probability with increasing distance is higher for fading in comparison to shadowing.

Interestingly, by comparing Figures 3(b) and 3(c), and Figures 4(b) and 4(c), we observe that as ρ increases, the delay increases for the same values of C and p. This is because as we only model the single request case, greedy opportunistic routing fails to take advantage of good channel, but requires a node to transmit multiple times over a bad channel. This need

This article has been accepted for publication in a future issue of this journal, but has not been fully edited. Content may change prior to final publication. Citation information: DOI 10.1109/TVT.2018.2880158, IEEE Transactions on Vehicular Technology

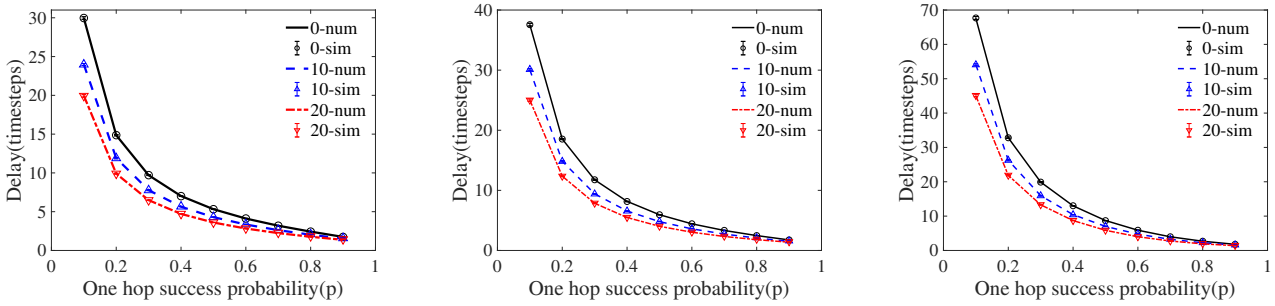

(a) Rayleigh Fading (Uncorrelated) (b) Rayleigh Fading ($\rho = 0.6$) (c) Rayleigh Fading ($\rho = 0.9$)

Fig. 3: Rayleigh Fading Channel

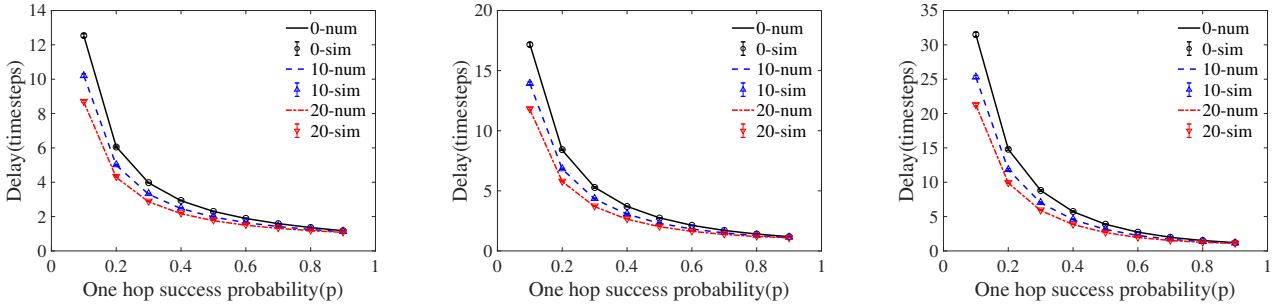

(a) Shadowing (Uncorrelated) (b) Shadowing ($\rho = 0.6$) (c) Shadowing ($\rho = 0.9$)

Fig. 4: Shadowing Channel

to transmit multiple times over a bad channel causes higher values of ρ to have a greater impact on delay, in particular for lower values of p ($p < 0.5$).

2) Impact of Network Parameters on Delay: We next investigate the impact of varying the network parameters on delay via numerical evaluation that utilizes the Markovian model. In Figure 5(a), we study the variation of the one hop success probability as the standard deviation (σ) of shadowing varies. We identify three classes of $\beta^{'}$ that impact the one hop success probability very differently. We note that when $\beta^{'} < 0$, the one hop success probability (p) is greater than 0.5, and when $\beta^{'} > 0$, p is less than 0.5. When $\beta^{'} = 0$, we observe that $p = 0.5$. As σ tends to infinity, p tends to 0.5 for all values of $\beta^{'}$. This is also evident from equation 5. The reason is that when σ tends to infinity, the bell curved nature of the normal distribution becomes a line, indicating that there are infinitely many shadowing values that affect successful and failed transmissions resulting in p = 0.5.

Figures 5(b) and 5(c) represent the variation in delay with σ. Comparing between Figures 5(b) and 5(c), it is evident that the delay decreases as the caching capacity increases. From the figures it is clear that variations in σ have a disproportional impact on delay with respect to the three classes of $\beta^{'}$ described above. We note that for $\beta^{'} > 0$, the delay is highly sensitive to variations in σ compared with the other two classes. The main reason is that for small values of σ, the one hop success probability is low in the $\beta^{'} > 0$ regime, thus resulting in high values of delay. The figure also demonstrates that if $\beta^{'} \leq 0$ (i.e., $p \geq 0.5$), then the overall performance is robust to changes in σ. We also observe that as σ increases,

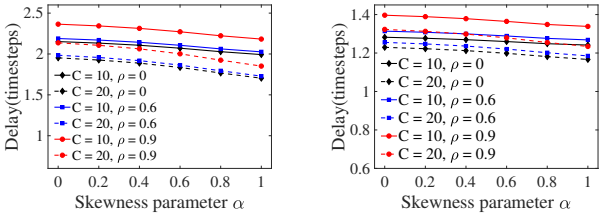

(a) Rayleigh Fading (b) Shadowing

Fig. 6: Delay vs. Zipfian Skewness Parameter (a)

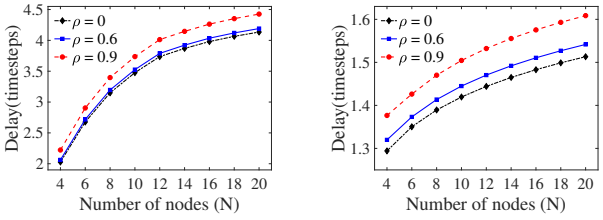

(a) Rayleigh Fading (b) Shadowing

Fig. 7: Delay vs. Number of Nodes (N)

the delay decreases and increases in the $\beta^{'} > 0$ and $\beta^{'} < 0$ regimes respectively. The primary reason is that as σ increases, the value of p decreases and increases to 0.5 for $\beta^{'} > 0$ and $\beta^{'} < 0$ respectively (as evidenced in Figure 5(a)).

Another important inference that one can make from the figures is that there is less utility in employing opportunism in

This article has been accepted for publication in a future issue of this journal, but has not been fully edited. Content may change prior to final publication. Citation information: DOI 10.1109/TVT.2018.2880158, IEEE Transactions on Vehicular Technology

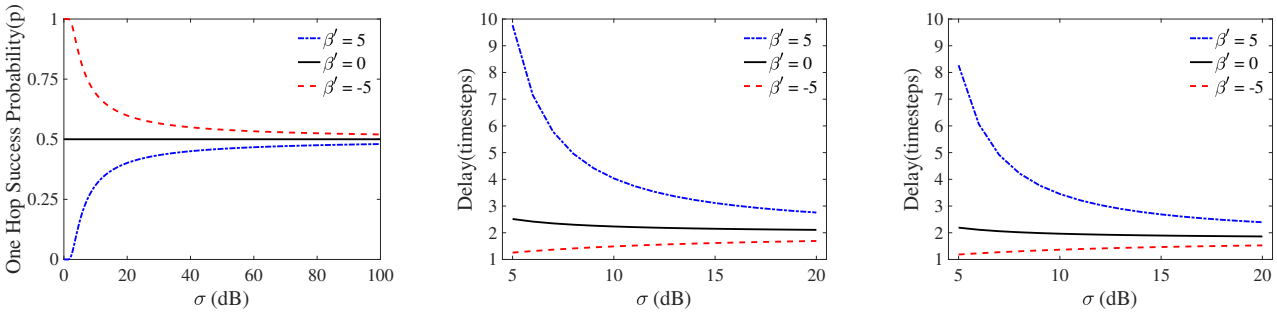

(a) One Hop Success Probability (p) vs Sigma (σ) (b) Delay vs Sigma (σ) (C = 10) (c) Delay vs Sigma (σ) (C = 20)

Fig. 5: Impact of Variance in Shadowing on Delay

an environment where σ takes large values. As $\beta^{'}$ is dependent on distance, it is clear that its value will vary between different node pairs. However, irrespective of the value of $\beta^{'}$ for high σ values, the probability of successful transmission between any two network nodes including one-hop transmission probability will tend to 0.5.

Figure 6 shows the variation in delay as the Zipfian skewness parameter changes. For the uncorrelated and correlated cases, we observe that the delay decreases as a increases, irrespective of the cache capacity. Note that incrementing a increases the skewness of the Zipfian distribution. When $a = 0$, the Zipfian distribution converges to a uniform distribution, while high values of a indicates that some pieces of content are considerably more popular in comparison to majority of content. The content placement strategy considered in our evaluation caches popular content with a higher probability. Therefore, for higher values of a, the probability of a request getting satisfied at an in-network cache increases, thereby resulting in lower delay. Once again, we observe that the delay increases as ρ increases.

Figure 7 shows the variation in delay as the number of network nodes increases considering Rayleigh fading and shadowing channels. We observe that as the number of nodes increases, the delay increases. This is expected because the average number of transmissions needed to reach the custodian or an en route cache having a copy of the content increases with the number of nodes. We also conduct experiments by increasing size of the content universe. For a fixed ratio of cache size to content universe size, we observe similar delay values, irrespective of content universe.

B. Trace based Evaluation

For conducting the trace-based evaluation, we use signal strength measurement traces collected over a wireless sensor network testbed by researchers at University of Duisburg-Essen, Germany and Norwegian University of Science and Technology, Norway [10]. The trace data includes packet delivery performance metrics collected under various parameter configurations for a period of 6 months between November 2012 and November 2013.

1) Trace Experiment Setup: We identify that data needed for experimentally validating greedy opportunistic forwarding must adhere to certain criteria. In particular, for each node, one-to-many transmissions must be recorded at each time interval and the nodes themselves must be ordered according to distance. We considered several publicly available traces, but we only found one trace [10] that could be directly mapped to the analyzed network model. For the purpose of these trace-based experiments, we consider a network of 4 nodes as shown in Figure 9 and map signal strength measurements (RSSI) collected at distances 10m, 20m and 30m to 7 channels in all. As depicted in Figure 9, there are 4, 2 and 1 channels at a distance of 10m, 20m and 30m respectively. In our experiments r_1 is the source while r_4 is the custodian.

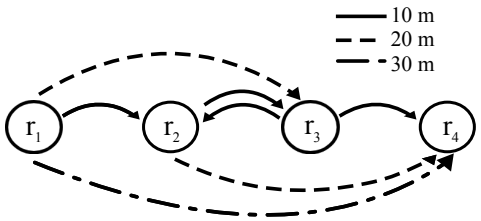

Fig. 9: Mapped Network model for Trace

For each distance the trace contains received signal strength information for successful transmissions for multiple transmission power levels between 3 and 31. These transmission power levels correspond to a power range between -25 dBm to 0 dBm respectively. The trace contains 300 successive requests for over 8000 iterations for each distance. In our experiments, a recorded RSSI value is considered as a successful transmission (mapped as 1) and the absence of a recorded value is considered as an unsuccessful transmission (mapped as 0). The mapping thus represents the channel quality in a binary fashion, as either good (1) or bad (0).

We note that the environment and the testbed from which these traces were collected may not necessarily correspond to a Rayleigh fading or shadowing environment. Therefore, in these trace-based experiments, to compare the performance of the proposed Markovian model for analyzing opportunistic routing via simulation and numerical evaluation we adopt the following approach. The simulations are carried out by considering the mapped trace data as results for transmission success and failure between different node pairs. For the numerical evaluation, the transmission probabilities values are computed using the empirical approach outlined in Section

This article has been accepted for publication in a future issue of this journal, but has not been fully edited. Content may change prior to final publication. Citation information: DOI 10.1109/TVT.2018.2880158, IEEE Transactions on Vehicular Technology

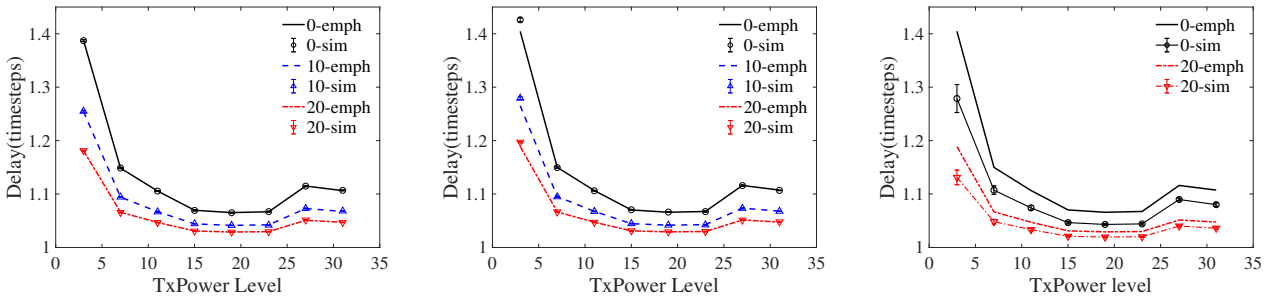

(a) Uncorrelated Channel (b) Correlated Channel (c) Correlated Channel(relaxed assumptions)

Fig. 8: Delay vs. TxPower Level

IV-C. For simulation and numerical evaluation, 100000 requests are generated according to a Zipfian distribution over 10 runs and the delay is calculated as the average number of hops needed for a hit considering all the requests. The error is calculated as the standard deviation for delay from the 10 runs of the experiment.

2) Trace Experiment Results: We note that real-world traces exhibit correlation between successive packet transmissions. Therefore, to emulate an uncorrelated channel using these traces, we first generate a random permutation of the trace. For the correlated channel experiments, we use the original trace without any alteration. Our model relies on the assumption that every time the source transmits a new packet, it obtains an i.i.d. channel. Therefore, for the correlated channel experiments, for a new packet transmission from the source, we select a channel quality uniformly at random from the trace and then consider channel correlation by selecting the subsequent channel fades sequentially.

Figures 8(a) and 8(b) show the delay for the uncorrelated and correlated channels using these traces for different power levels. The increment in power level generally corresponds to an increase in the probability of a direct successful transmission between any two pair of nodes and thus the delay decreases. We observe that a sudden increase in delay occurs for power levels greater than 27 for both uncorrelated and correlated channels. Fu *et al.* [11] observe a higher number of failures in the trace data for larger distances (i.e., including the direct link between the source and the custodian). They attribute this behavior to increased mobility in the surrounding. Additionally, the trace data [10] contains a higher number of failures, particularly for larger power levels of 27 and 31, thus resulting in increased delay.

We once again observe from Figures 8(a) & 8(b) that the simulation and numerical results match closely that demonstrates the widespread applicability of our model. We note that though the numerical values in both Figures 8(a) and 8(b)) are close, we observe that similar to the results obtained in Figures 3 and 4, the delay for correlated channels is higher than uncorrelated channels. We also observe from the trace that except for power levels 3 and 7, the calculated transmission probabilities are high on average and lie within 0.8 and 1.0. Therefore, significant number of transmissions result in a success, and so the delay values for the uncorrelated and correlated channels are close to each another for the other power levels.

3) Discussion on the Markovian channel and i.i.d. assumption: In this subsection, we investigate the impact of the following assumptions—*i)* the channel correlation can be completely captured via a Markovian model, and *ii)* whenever the source transmits a new packet, it gets an i.i.d. channel. The i.i.d. assumption is closely tied to the correlated channel being Markovian because as we consider only a single packet in transit, a successful transmission erases the memory of the channel. From the trace, we observe that successes and failures tend to occur in bursts, thus violating the Markovian channel assumption.

We observe from Figure 8(b) that there is a difference in delay between the numerical and simulation results for power level 3. We hypothesize that this difference is primarily due to the violation of the Markovian channel assumption. We note that power level 3 has the largest number of successive failures, and thus has the highest possibility of violating the Markovian assumption. Figure 8(c) compares the simulation and numerical results with the i.i.d. assumption relaxed in the simulation. In these simulations instead of picking the first transmission of a new packet randomly, the values were picked in order. As expected, no difference is observed in the numerical results between figures 8(b) and 8(c).

In contrast, the simulated delays for 8(c) show a decrease in delay for all power levels and cache capacities. The decrease in simulated delay can be attributed to the nature of the spread among the failed and successful transmissions. Failed transmissions tend to occur together followed by large number of uninterrupted successful transmissions. Therefore, though some packets incur large delays due to these transmission failures, majority of the packets incur lower delays, resulting in reduced delay overall. We observe that even though the numerical and simulation results do not match closely in this setting, our Markovian model for analyzing opportunistic forwarding is successful in capturing the trend in the delay variation. We plan to analyze opportunistic routing for channels with significant memory as part of our future research.

VII. Conclusion

In this paper, we analyzed the delay of opportunistic request routing in cache-enabled wireless networks. To this end, we

designed Markovian models and derived expressions for the transition probabilities considering uncorrelated and temporally correlated wireless channels. We then utilized the steady state probabilities of the Markov chain to determine expressions for the request routing delay. Via numerical evaluation and simulation, we demonstrated the validity and effectiveness of our Markovian models in modeling the request routing delay. In future, we plan to extend this work for more realistic scenarios by considering pipelined request streams and interference from multiple competing flows. Additionally, as network size increases, the Markovian model developed in this paper is likely to encounter a state space explosion. Therefore, we plan to develop approximate algorithms to address this issue as part of our future work.

REFERENCES

[1] S. Biswas and R. Morris. Exor: opportunistic multi-hop routing for wireless networks. *ACM SIGCOMM Computer Communication Review*, 35(4):133–144, 2005.

[2] S. H. Chae and W. Choi. Caching placement in stochastic wireless caching helper networks: Channel selection diversity via caching. *IEEE Transactions on Wireless Communications*, 15(10):6626–6637, 2016.

[3] N. Chakchouk. A survey on opportunistic routing in wireless communication networks. *IEEE Communications Surveys & Tutorials*, 17(4):2214–2241, 2015.

[4] C.-K. Chau, A. Seetharam, J. Kurose, and D. Towsley. Opportunism vs. cooperation: Comparing forwarding strategies in multihop wireless networks with random fading. In *Communication Systems and Networks (COMSNETS), 2013 Fifth International Conference on*, pages 1–10. IEEE, 2013.

[5] W. Chen, C.-T. Lea, S. He, and Z. XuanYuan. Opportunistic routing and scheduling for wireless networks. *IEEE Transactions on Wireless Communications*, 16(1):320–331, 2017.

[6] K.-C. Chung, W.-H. Kuo, and W. Liao. Delay analytical models for opportunistic routing in wireless ad hoc networks. *IEEE Transactions on Vehicular Technology*, 66(6):5330–5339, 2017.

[7] R. W. Coutinho and A. Boukerche. Opportunistic routing in underwater sensor networks: Potentials, challenges and guidelines. In *Distributed Computing in Sensor Systems (DCOSS), 2017 13th International Conference on*, pages 1–2. IEEE, 2017.

[8] A. Darehshoorzadeh, E. Robson, and A. Boukerche. Toward a comprehensive model for performance analysis of opportunistic routing in wireless mesh networks. *IEEE Transactions on Vehicular Technology*, 65(7):5424–5438, 2016.

[9] M. Dehghan, A. Seetharam, B. Jiang, T. He, T. Salonidis, J. Kurose, D. Towsley, and R. Sitaraman. On the complexity of optimal routing and content caching in heterogeneous networks. In *Computer Communications (INFOCOM), 2015 IEEE Conference on*, pages 936–944. IEEE, 2015.

[10] S. Fu and Y. Zhang. CRAWDAD dataset due/packet-delivery (v. 2015-04-01). Downloaded from https://crawdad.org/due/packet-delivery/20150401, Apr. 2015.

[11] S. Fu, Y. Zhang, Y. Jiang, C. Hu, C.-Y. Shih, and P. J. Marrón. Experimental study for multi-layer parameter configuration of wsn links. In *Distributed Computing Systems (ICDCS), 2015 IEEE 35th International Conference on*, pages 369–378. IEEE, 2015.

[12] M. Gudmundson. Correlation model for shadow fading in mobile radio systems. *Electronics letters*, 27(23):2145–2146, 1991.

[13] M. Ji, G. Caire, and A. F. Molisch. Wireless device-to-device caching networks: Basic principles and system performance. *IEEE Journal on Selected Areas in Communications*, 34(1):176–189, 2016.

[14] S. M. Kim, S. Wang, and T. He. Exploiting causes and effects of wireless link correlation for better performance. In *Computer Communications (INFOCOM), 2015 IEEE Conference on*, pages 379–387. IEEE, 2015.

[15] N. Li, J.-F. Martinez-Ortega, V. H. Diaz, and J. A. S. Fernandez. Probability prediction based reliable opportunistic (pro) routing algorithm for vanets. *arXiv preprint arXiv:1709.08199*, 2017.

[16] T. S. Rappaport. Wireless communications–principles and practice, (the book end). *Microwave Journal*, 45(12):128–129, 2002.

[17] E. Rozner, J. Seshadri, Y. Mehta, and L. Qiu. Soar: Simple opportunistic adaptive routing protocol for wireless mesh networks. *IEEE transactions on Mobile computing*, 8(12):1622–1635, 2009.

[18] A. Seetharam and J. Kurose. An analysis of opportunistic forwarding for correlated wireless channels. In *World of Wireless, Mobile and Multimedia Networks (WoWMoM), 2015 IEEE 16th International Symposium on a*, pages 1–3. IEEE, 2015.

[19] A. Seetharam, J. Kurose, and D. Goeckel. A markovian model for coarse-timescale channel variation in wireless networks. *IEEE Transactions on Vehicular Technology*, 65(3):1701–1710, 2016.

[20] K. Shanmugam, N. Golrezaei, A. G. Dimakis, A. F. Molisch, and G. Caire. Femtocaching: Wireless content delivery through distributed caching helpers. *IEEE Transactions on Information Theory*, 59(12):8402–8413, 2013.

[21] W.-Y. Shin, S.-Y. Chung, and Y. H. Lee. Parallel opportunistic routing in wireless networks. *IEEE Transactions on Information Theory*, 59(10):6290–6300, 2013.

[22] H. Wang, Y. Liu, and S. Xu. An opportunistic routing protocol based on link correlation for wireless mesh networks. In *Wireless Communications, Networking and Applications*, pages 113–125. Springer, 2016.

[23] S. Wang, A. Basalamah, S. M. Kim, S. Guo, Y. Tobe, and T. He. Link-correlation-aware opportunistic routing in wireless networks. *IEEE Transactions on Wireless Communications*, 14(1):47–56, 2015.

[24] J. Wu, S. Affes, and P. Mermelstein. Forward-link soft-handoff in cdma with multiple-antenna selection and fast joint power control. *IEEE transactions on wireless communications*, 2(3):459–471, 2003.

[25] C. Yang, Y. Yao, Z. Chen, and B. Xia. Analysis on cache-enabled wireless heterogeneous networks. *IEEE Transactions on Wireless Communications*, 15(1):131–145, 2016.

[26] Y. Zhang, J. Zhang, D. Dong, X. Nie, G. Liu, and P. Zhang. A novel spatial autocorrelation model of shadow fading in urban macro environments. In *Global Telecommunications Conference, 2008. IEEE GLOBECOM 2008. IEEE*, pages 1–5. IEEE, 2008.

[27] Z. Zhao, W. Dong, G. Guan, J. Bu, T. Gu, and C. Chen. Modeling link correlation in low-power wireless networks. In *Computer Communications (INFOCOM), 2015 IEEE Conference on*, pages 990–998. IEEE, 2015.

[28] M. Zorzi, R. Racd, and L. B. Milstein. A markov model for block errors on fading channels. In *Personal, Indoor and Mobile Radio Communications, 1996. PIMRC'96., Seventh IEEE International Symposium on*, volume 3, pages 1074–1078. IEEE, 1996.

[29] M. Zorzi, R. R. Rao, and L. B. Milstein. Arq error control for fading mobile radio channels. *IEEE Transactions on Vehicular Technology*, 46(2):445–455, 1997.

J. Dinal Herath is a graduate student in the computer science department at State University of New York Binghamton. He received his Bachelor of Science degree from Department of Physics, University of Colombo, Srilanka. His research interests include computer networks, wireless networks and cache networks.

Anand Seetharam is an assistant professor in the computer science department at State University of New York Binghamton. He obtained his PhD. from University of Massachusetts Amherst in 2014. He is broadly interested in the field of computer networking. His research encompasses internet-of-things, information-centric networks, wireless networks, and security. He has published numerous papers in peer-reviewed journals and conferences. He co-organized the IEEE INFOCOM 2016 MuSIC workshop and the IEEE MASS 2015 CCN workshop. He has served on the TPC of multiple conferences including IEEE ICC, IEEE ICCCN and IEEE WoWMoM and as reviewer for multiple journals including IEEE TMC, IEEE TNET and Computer Networks. He has won multiple awards including the ACM ICN 2014 runners up to best paper award, the University of Massachusetts Amherst Outstanding Synthesis Award and the University of Massachusetts Amherst Portfolio with Distinction Award and has a U.S. patent on video streaming systems.